The Ability of MM5 to Simulate Ice Clouds: Systematic Comparison between Simulated and Measured Fluxes and Lidar/Radar Profiles at SIRTA Atmospheric Observatory

M. Chiriaco, R. Vautard, H. Chepfer, M. Haeffelin, Y. Wanherdrick, Y. Morille
Institut Pierre Simon Laplace
Laboratiore de Météorologie Dynamique
Palaiseu, France

A. Protat
Institut Pierre Simon Laplace
Centre d'études des Environnements Terrestre et Planétaires
Paris, France

J. Dudhia
National Center for Atmospheric Research
Boulder, Colorado

Introduction

Ice clouds play a major role in the radiative energy budget of the Earth-atmosphere system (Liou 1986). Their radiative effect is governed primarily by the equilibrium between their albedo and greenhouse effects. Both macrophysical and microphysical properties of ice clouds regulate this equilibrium. For quantifying the effect of these clouds onto climate and weather systems, they must be properly characterized in atmospheric models.

In this paper we use remote-sensing measurements from the SIRTA ground based atmospheric observatory (Site Instrumental de Recherche par Télédétection Atmosphérique, http://sirta.lmd.polytechnique.fr). Lidar and radar observations taken over 18 months are used, in order to gain statistical confidence in the model evaluation. Along this period of time, 62 days are selected for study because they contain parts of ice clouds. We use the "model to observations" approach by simulating lidar and radar signals from MM5 outputs. Other more classical variables such as shortwave and longwave radiative fluxes are also used.

Four microphysical schemes, among which that proposed by Reisner et al. (1998) with original or modified parameterizations of particle terminal fall velocities (Zurovac-Jevtic and Zhang 2003, Heymsfield and Donner 1990), and the simplified Dudhia (1989) scheme are evaluated in this study.

MM5 Model Simulations

The MM5 model domain covers Northern France and consists in 2 nested grids, the coarsest resolution being of 15 km and the finest of 5 km. The two-way nesting method is used. The finest grid, which is that from which cloud fields are eventually extracted for the present study, covers about 200 x 200 km² around Paris. At the boundaries of the coarse domain, MM5 is forced by the National Center for Environmental Prediction (NCEP) 1° x 1° analyses provided every 6 hr. We choose a vertical setup of 61 layers from the ground to the 100-hPa top surface. Model layers are about 200-400 m thick in the upper troposphere where ice clouds reside.

We use the classical MM5 parameterizations, proposed as options in the MM5 configuration file, with the following modifications. Regarding convection, the Grell (1993) scheme is used. Turbulence in the planetary boundary layer is parameterized using the Medium Range Forecast scheme (MRFPBL), mostly borrowed from the Troën and Mahrt (1986) approach. According to Liu (2004), the original calculation of the friction velocity uses an unrealistic convective velocity parameterization. As suggested by this author, the convective velocity formulation is replaced by the Beljaars (1994) formulation. The NOAH (Newcastle Object-oriented Advanced Hydroinformatics) land surface model is used. Atmospheric radiation transfer uses the optional CCM2 (NCAR Community Climate Model, Hack et al. 1993) scheme, with a modification on assumed fixed effective ice particle diameter (35 μm) instead of 14.6 μm in the original routine, which is a more realistic value (Liou 2002).

Our intention is to evaluate and compare several microphysical schemes. Four schemes that are available as MM5 options or variants, are used (Table 1).

Table 1. Description of the 4 microphysical schemes used in MM5.		
Name of the Scheme	**Reference of the Parameterization**	**Ice Particles Sedimentation Velocity**
A	Reisner et al. 1998 option 5 - $N_{S,ice}$ predicted	Zurovac-Jevtic and Zhang 2003: $V_{S,fall}(z) = a.[q_{S,ice}(z).\rho_{air}(z)]^b$ - if $q_{S,ice}(z).\rho_{air}(z) \leq 4.8.10^{-6}$: $a = 180.65$ and $b = 0.52$ - else: $a = 3.13$ and $b = 0.19$
B	Reisner et al. 1998 option 5 - $N_{S,ice}$ predicted	Heymsfield and Donner 1990: $V_{S,fall}(z) = a[q_{S,ice}(z).\rho_{air}(z)]^b$ $a = 3.29$ and $b = 0.16$
C	Reisner et al. 1998 option 5 - $N_{S,ice}$ predicted	Reisner et al. 1998 $V_{S,fall}(z) = 700 \times 2r_{S,ice}(z)$
D	Simple Ice, Dudhia 1989 no prediction of $N_{S,ice}$ *distinction between ice and liquid usinsa* *temperature threshold: $T_t=20°C$*	Heymsfield and Donner 1990: $V_{S,fall}(z) = a[q_{S,ice}(z).\rho_{air}(z)]^b$ $a = 3.29$ and $b = 0.16$

Observations

The SIRTA provides routine observations of the atmospheric column (Haeffelin et al. 2004):

1) *A ground-based 532-nm lidar*. It operates 4 days a week except when it is raining. The temporal resolution is 10 seconds, and the vertical resolution is 15 m. It is a zenith viewing lidar that measures both the backscattered signal and linear depolarization ratio. The lidar signal is normalized to the molecular. The phase is deduced from lidar depolarization ratio (Sassen 1991, Noel et al. 2001) that is normalized to 2.8% in a molecular portion of the atmosphere. In presence of clouds, ratios lower than 5% are associated to liquid water, and ratios larger than 20% to ice and/or snow. When ratio ranges between 5 and 20%, the cloud is classified as having a mixed phase.

2) *A ground-based 95-GHz radar*. It operates continuously since October 2002. Data are acquired with a 1 second temporal resolution and vertical resolution is 60 m. The reflectivity and Doppler velocity are obtained from 0.2 to 15 km. The radar sensitivity is ~ -50 dBZ at 1 km and it looses $20 \times \log(z_{km})$ of sensitivity every km.

3) *Radiative flux station*. The Pyrheliometer measures the direct shortwave flux $SW_{dct,M}$ and the Pyranometer measures the diffuse shortwave flux $SW_{dff,M}$. The Pyrgeometer measures the net longwave flux $LW_{n,M}$.

Sixty-two cloudy days have been selected based on lidar and radar observations. Days with observed only low-level liquid clouds or only clear sky periods were removed by a visual inspection of the observations. When lidar observations are available, ice/snow cloud cases are selected when the lidar depolarization profiles contain values larger than 10%. When only radar observations are available, a cloud case is selected only when a high altitude cloud layer (typically 8-10 km) is present during the day, event if it does not persist all day long.

The ACTSIM Model to Observation Comparison Method

In order to compare model and observations, comparisons of lidar, radar profiles and vertical velocity require a post-processing of model outputs. We developed a post-processing program package called ACTSIM (ACTive remote-sensing SIMulator).

For A-, B- and C-schemes, ice number concentration is available and the snow and ice particle effective radii $r_{S,snow/ice}(z)$ are deduced from the microphysical scheme (Table 2). For the 4 schemes, liquid water particle effective radius $r_{S,liq}$ is constant (10 μm) in ACTSIM, which allows to derive $N_{S,liquid}(z)$ from $r_{S,liquid}$ and $q_{S,liquid}(z)$ (prognostic variable).

Table 2. Differences between the 4 schemes concerning ACTSIM calculation. $\rho_{S,ice/snow}$ is the simulated density of ice/snow (500 kg.m^{-3}/100 kg.m^{-3}) for A-, B- and C-schemes.

	$N_{S,ice}$	$N_{S,snow}$	$r_{S,ice}$	$r_{S,snow}$
A, B, C	predicted	$\dfrac{N_{0,S,snow}^{3/4}}{\left(\dfrac{\rho_{air}q_{S,snow}}{\rho_{snow}\pi}\right)^{1/4}}$, $N_{0,S,snow}$ variable	$\left(\dfrac{3q_{S,ice}\rho_{air}}{N_{S,ice}4\pi\pi_{ice}}\right)^{1/3}$	$\left(\dfrac{3q_{S,snow}\rho_{air}}{N_{S,snow}4\pi\pi_{snow}}\right)^{1/3}$
D	$\dfrac{3q_{S,ice}\rho_{air}}{4\pi\pi_{S,ice}^{3}\rho_{ice}}$	$\dfrac{N_{0,S,snow}^{3/4}}{\left(\dfrac{\rho_{air}q_{S,snow}}{\rho_{snow}\pi}\right)^{1/4}}$, $N_{0,S,snow}$ fixed 2.10^{7}m^{-4}	fixed value: 30 µm	$\left(\dfrac{3q_{S,snow}\rho_{air}}{N_{S,snow}4\pi\pi_{snow}}\right)^{1/3}$

In order to simulate lidar and radar profiles as realistic as possible, we consider a size distribution in ACTSIM. For ice and liquid water, we use a log-normal distribution with a modal radius equal to $r_{S,ice/liquid}$:

$$n_{S,ice/liquid}(z,\Re).d\Re = \frac{N_{S,ice/liquid}(z)}{\sqrt{2\pi}\Re.\ln\sigma}.e^{-\frac{\ln^2\left(\frac{\Re}{r_{S,ice/liquid}(z)}\right)}{2\ln^2\sigma}}.d\Re \tag{1}$$

where $n_{S,ice/liquid}(z,\Re).d\Re$ is the number of particles of ice/liquid that have an effective radius between $\Re$ and $\Re + d\Re$. The σ value is constant and equal to 1.2 for ice clouds (Heymsfield and Platt 1984). The values of $\Re$ vary between $\Re_{min} = 0.27 \times r_{S,ice/liquid}(z)$ (11 µm) and $\Re_{max} = 3.44 \times r_{S,ice/liquid}(z)$ (140 µm). The shape of the snow size distribution is a Marshall-Palmer size distribution:

$$n_{S,snow}(z,\Re).d\Re = N_{0,S,snow}(z).e^{-\frac{\Re}{2}\left(\frac{\pi\rho_{snow}N_{0,S,snow}(z)}{\rho_{air}q_{S,snow}(z)}\right)^{1/4}}d\Re \tag{2}$$

where $n_{S,snow}(z,\Re).d\Re$ is the number of particles of snow that have an effective radius between $\Re$ and $\Re + d\Re$.

The 532-nm lidar equation giving the backscattered signal power is:

$$P_S(z)z^2 = \left(\beta_{mol}(z) + \beta_{S,par}(z)\right).e^{-2\int_0^z\left[\eta.\alpha_{S,par}(z)+\alpha_{mol}(z)\right]dz} \tag{3}$$

where $P_S(z)z^2$ is the simulated lidar backscattered normalized signal at the altitude z.

The simulated particle attenuation by scattering $\alpha_{S,par}(z)$ in m^{-1} is the sum of the contribution of snow, liquid water and ice water. The particle scattering efficiency Q is equal to 2 at 532 nm because particles of snow, ice and liquid water are much larger than the lidar wavelength (Ulaby et al. 1943). Furthermore, the η term in (3) is a multiple scattering correction parameter that is taken equal to 0.5 (Platt 1973). $\beta_{S,par}(z)$ is the simulated lidar backscattering coefficient by particles and is the sum of the contribution of snow, ice and liquid water:

$$\beta_{S,\text{snow/ice/liquid}}(z) = \frac{P_{S,\pi,\text{snow/ice/liquid}}(z)}{4\pi}\alpha_{S,\text{snow/ice/liquid}}(z) \tag{4}$$

where $P_{S,\pi,\text{snow/ice/liquid}}(z)$ is the simulated scattering phase function in backscattering. In the four microphysical schemes, particles are assumed to be spherical, hence, in order to be consistent with the model assumptions, $P_{S,\pi,\text{snow/ice/liquid}}(z)$ is computed with Mie theory for the size distributions given in (1) and (2). $\beta_{mol}(z)$ is the lidar backscattering coefficient by molecules and depends on temperature $T(z)$ and pressure $p(z)$ profiles (Collis and Russel 1976).

Every values of radar reflectivity $ZdB_S(z)$ that are inferior to $-50+20\log(z)$ are eliminated because of the radar sensitivity. $Z_{S,\text{snow/ice/liquid}}(z)$ is the contribution of snow/ice/liquid to the simulated radar reflectivity:

$$Z_{S,\text{snow/ice/liquid}}(z) = \int_{\Re_{min}}^{\Re_{max}} \left(2\Re.10^3\right)^6 . n_{S,\text{snow/ice/liquid}}(z,\Re).d\Re \tag{5}$$

The radar reflectivity is calculated using the size distributions described in Section 4.1.

The Doppler velocity $V_s(z)$ (m.s^{-1}) measured by the vertically-pointing radar is the sum of the vertical velocity of air $w_S(z)$ and the terminal velocity $V_{S,t}(z)$ of the ice particles. For each scheme, $V_{S,t}(z)$ is calculated using Eq. given in Table 1.

Statistical Analysis: Hourly Sampled Data, Observations 10 Minute Averages Every Hour

Cloud Occurrence, Life-Time and Thermodynamical Phase

The Morille et al. (2005) algorithm is applied for both observations and simulations and hits and misses are counted for each microphysical option. Figure 1a shows the rates of cloud hits, non detection and false alarm. For the 4 schemes, simulated and measured clouds match in more than 65% of cases, and this agreement is maximal for Scheme D (the "simple ice" scheme), with a hit rate of about 75%. All schemes overestimate the cloud occurrence in about 20% of cases (25% for Scheme C, the original Reisner et al. [1998] scheme). Scheme B (Reisner et al. [1998] with the Heymsfield and Donner [1990] terminal velocity) is the most balanced scheme.

In order to study the life time of clouds, 15 days corresponding to persistent homogeneous cloud layers where beginning and end of cloud is observed have been subjectively selected. Figure 1b shows the Probability Density Function (PDF) of the difference between the simulated and the measured cloud life time. In the 4 schemes, the tendency is to simulate longer life time than the observed one, and the maximal difference is more than 6 hours found in 20% of cases whatever the scheme.
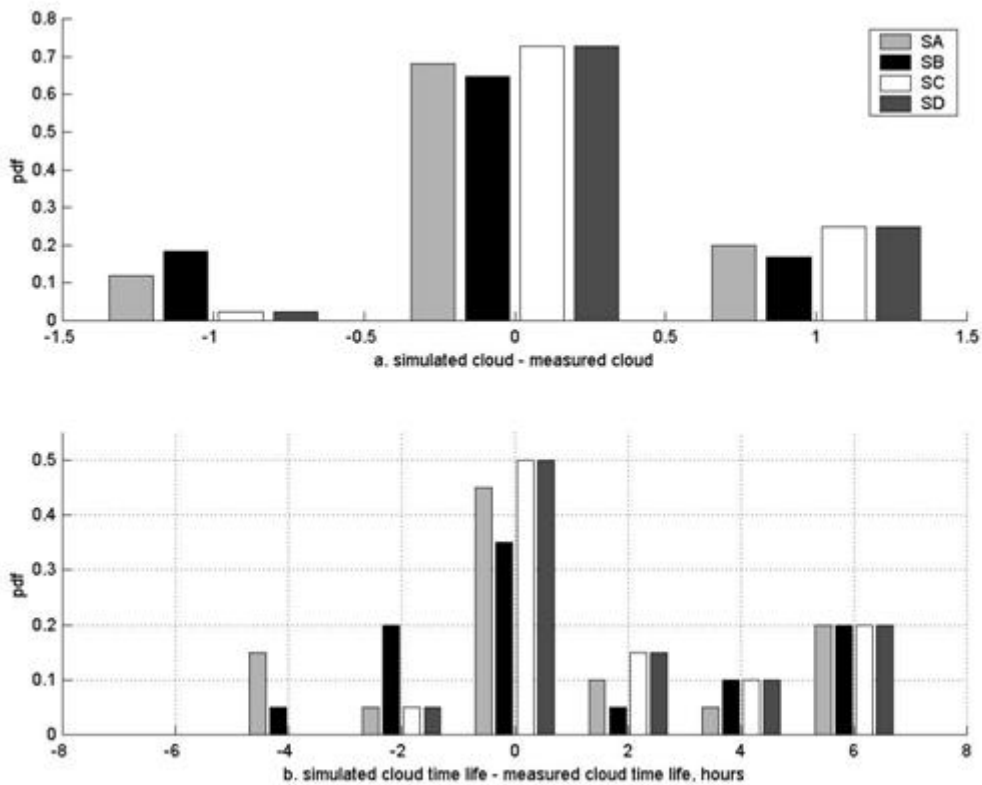
Figure 1. Sixty-two days statistical study about cloud occurrence and life time using lidar, one point every hour: (a) -1 value: simulated lidar does not detect any cloud whereas observed lidar detects one; 0 value: simulated lidar and observed lidar does agree concerning the presence of cloud; 1 value: simulated lidar detects a cloud whereas observed lidar does not detect any, (b) probability density function of the difference between the simulated and the measured cloud time life, as detected by lidar (hours). A-scheme is in light grey, B-scheme in black, C-scheme in white and D-scheme in dark grey.

For all the cases with available lidar measurements, simulated and measured thermodynamical phases are determined and compared at every hour and altitude, from lidar depolarization ratio for observations, and directly from output for simulations. Figure 2a shows the simulated cloud phase when the observed cloud is liquid water (i.e. 20% of the total lidar dataset): Scheme D with the -20° threshold gives the best phase estimation with 60% of liquid water, whereas the 3 other schemes produce ice and snow instead of liquid water in more than 80% of cases. Figure 2b corresponds to the observed mixed phase cloud (i.e. 40% of the total lidar dataset). The 4 schemes are not consistent with observation as they do not lead to a mix of liquid water and ice and/or snow. When the lidar depolarization ratio leads to ice and/or snow crystals (Figure 2c), the simulated phase is a snow and/or ice for almost 100% of cases for A-, B- and C-schemes and 80% for D-scheme. These results show that the Reisner et al. (1998) scheme generally overestimates the fraction of ice/snow in high clouds.
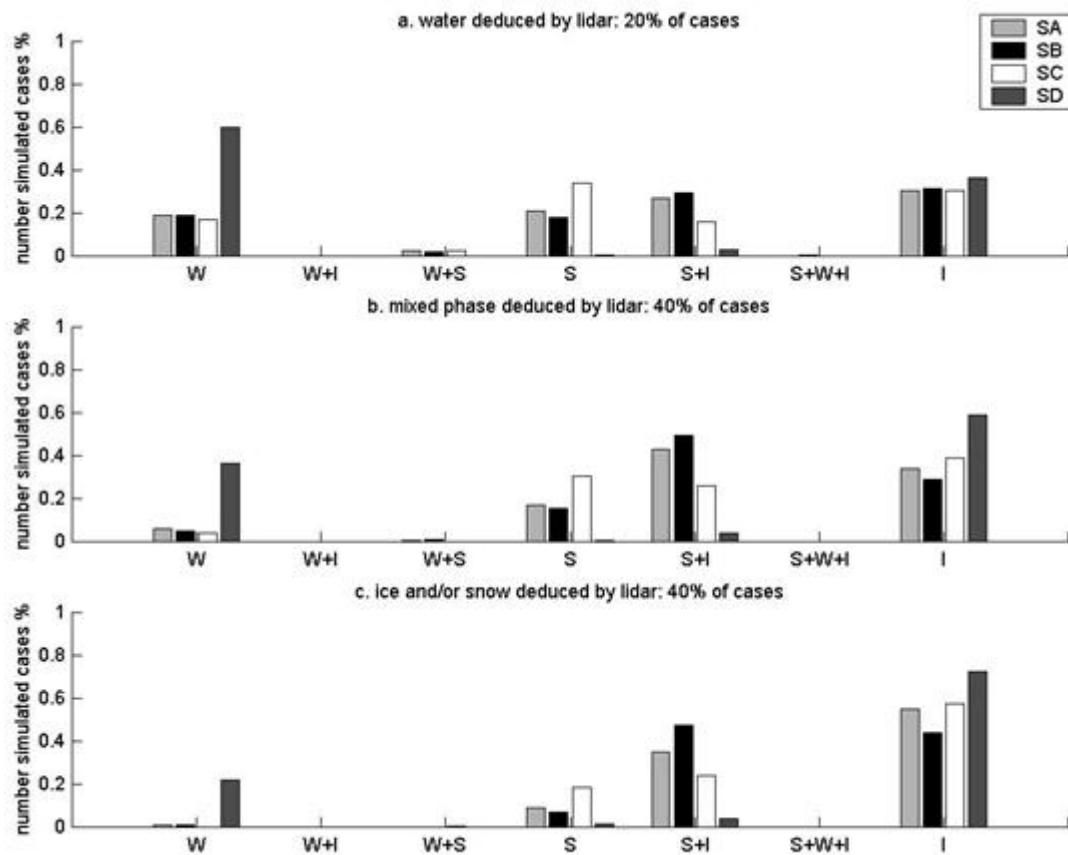
Figure 2. Sixty-two days statistical study about phase, one point every hour and every km: (a) simulated phase when measured lidar depolarization ratio leads to liquid water, (b) the same for mixed phase, (c) the same for ice. 'W' means liquid water, 'S' means snow, 'I' means ice. A-scheme is in light grey, B-scheme in black, C-scheme in white, and D-scheme in dark grey.

Lidar/Radar Profiles, Vertical Velocity and Radiative Fluxes

We have studied the correlation coefficients and the bias between simulations and measurements concerning the following parameters: lidar and radar integrated profiles, altitudes where lidar and radar signals are maximal within the cloud, vertical velocity where the radar signal is maximal, LongWave (LW) and ShortWave (SW) fluxes. Results are not precisely shown, but we here discuss interpretation. It shows that lidar integrated profile are hard to reproduce comparing to radar profiles, certainly because they correspond to thinner clouds.

There is a low bias in schemes A and B concerning the cloud altitude. It could be explained by the lack of differentiation between terminal velocities of small particles which should stay suspended in the upper part and big ones which should lie in the lower part. When applying a terminal velocity that does not depend on particle size (but on IWC), one overestimates the fall velocity of smaller particles and underestimate that of large ones. Consequently particles may artificially "accumulate" at the cloud bottom.

In one hand, simulated and measured altitudes of maximal radar reflectivity are in good agreement. It means that the model reproduces correctly the vertical distribution of particle size, because the radar reflectivity depends on particle radius at the first order. On the other hand, the lidar backscatter signal depends on both particle size and particle concentration number at the first order. Hence, the difference between simulated and measured maximal lidar signal is due to a biased representation of the vertical distribution of the particle concentration number.

Finally, comparisons between altitudes of lidar and radar maximum signals show that for both measurements and simulations, the radar maximum is located higher than the lidar one. This statement means that $z[P_S(z)z^2]_{max} < z[P_M(z)z^2]_{max} < z[ZdB_M(z)]_{max} < z[ZdB_S(z)]_{max}$. It then shows that the model overestimates the cloud vertical extends whatever the microphysical scheme.

The mean profiles of all profiles are shown for measurements and simulations in Figure 3. The shape of the curves show that for the four schemes, it is difficult to reproduce the lidar profile; nevertheless, the profile from scheme C is by the same order of magnitude than the measured one, but with a higher and more extended cloud. The simulated mean radar profiles using schemes A and B are closed to the measured one, in term of order of magnitude and in term of altitude, meaning that the vertical distribution of the particle size is good and so that the lidar discrepancies are mostly due to a problem of the vertical distribution of the particle concentration number. Furthermore, it is interesting to notice that the simple scheme D performs as well as schemes A and B.
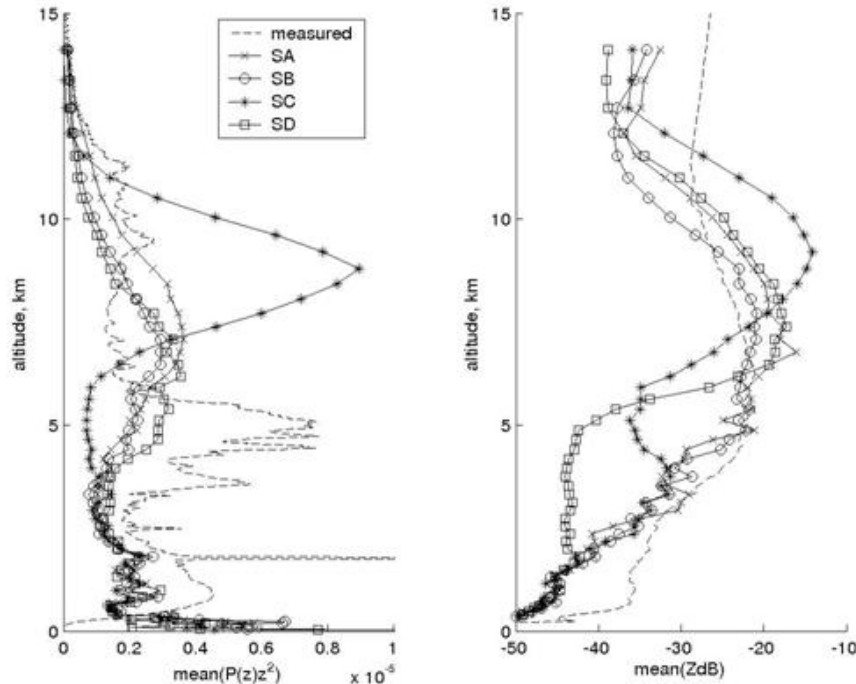

Figure 3. (a) Mean profile of all lidar profiles (every selected case every hour) for measurements in dashed line, for simulation using scheme A in plane line with cross, using scheme B in plane line with circle, using scheme C in plane line with star and using scheme C in plane line with square, (b) same as (a) for radar.

Concerning the vertical velocity Scheme B produces the best correlations. Because of the weak order of magnitude of w_S compared to $V_{S,t}$, general biases are mostly due to the difference between the simulated and the measured terminal velocities: simulated particles fall more slowly than observed ones. This is consistent with the earlier conclusion that the cloud life time was longer for simulations than for observations. However one should keep in mind that only the large particles in the particle size distribution can be seen by the radar and therefore the fall velocity of smaller, but more numerous particles is not accounted for. The discrepancies between simulations and observations are consistent with this possible effect. Even though scheme C appears to be the most physical (terminal fall velocity related to particle size), it reveals the largest bias with simulated velocities underestimated by 0.6 cm/s.

The skill in predicting cloud occurrence is reflected by the skill in predicting radiative fluxes. All schemes give similar correlation coefficients. However differences can be seen: the longwave flux is on average underestimated for all schemes (of about 10 $W.m^{-2}$). This could be either due to errors in simulated cloud properties or to clear sky simulated LWF bias, because the latter is known to be difficult to accurately simulate in atmospheric models. On the contrary, the simulated SWF is overestimated for all schemes except Scheme C. As the radiative code is the same for all model experiments, the discrepancy is due the microphysical scheme. For Schemes A, B and D, the longwave and shortwave fluxes behaviours are self-consistent and are in agreement with the lidar and radar integrated signals to show that the simulated cloud is not opaque enough.

Discussion and Conclusion

Table 3. Best microphysical scheme performance for each variable concerning the correlation coefficient, the mean value of the difference between simulations and measurements, and the tendency. "Simu" stands for simulations and "measu" for measurements.

	$R_{S/M}$ Best Scheme	Mean(simu-measu) Best Scheme	General Tendency
occurrence	—	B	too much occurrence for A, C and D B more equilibrate
time life	—	all equivalent	clouds too persistent
thermodynamical phase	—	all equivalent	too much ice and snow and not enough water
$[P(z).z^2]_{integrated}$	C	D	simu < measu except for C but "bad scores" for all schemes
$[ZdB(z)]_{integrated}$	A, B	B, D	simu < measu except for D
$z[P(z).z^2]_{max}$	A	C	simu < measu except for C
$z[ZdB(z)]_{max}$	D	A, B	simu > measu
$V[ZdB(z)]_{max}$	B	B	simu > measu
LW	all equivalent	all equivalent	simu < measu
SW	all equivalent	A	simu > measu except for C

The general tendencies are drawn in Table 3. In terms of systematic biases, all microphysics tend to produce clouds that are too persistent (occurrence and life time). Scheme B is the least biased scheme. The original scheme (C) has the strongest bias. The model tends to produce ice and snow instead of liquid water (thermodynamical phase), and when ice clouds are properly built, they tend to contain an insufficient quantity of ice/snow (integrated lidar and radar signals and SWF), i.e. to not be opaque enough. The cloud vertical extent is overestimated in the model.

The strong bias of the Reisner et al. (1998) scheme makes it difficult to use in practice. The small modifications of the velocities clearly improve the model results in terms of cloud occurrence and radiation. The "simple ice" scheme has striking skill given its degree of simplification, and has the advantage of being computer inexpensive but does not provide water phase characteristics.

Additionally information about the true microphysical properties (particle size and shape, density) would certainly help assess in which microphysical conditions MM5 model associated to Scheme B are most accurate. With this conclusion in mind, a microphysical study will be performed using the same type of measurements and adding ice cloud microphysical retrievals: ice particle shape retrieval using Noel et al (2002), ice particle size from lidar and IR radiometry (Chiriaco et al. 2004) and from radar (Protat et al. 2004), as well as liquid and ice water content and fluxes at the top of the atmosphere applied to the geostationary Meteosat Second Generation (MSG) satellite (Minnis et al. 1998). The approach presented in this paper will also be carried on using Aqua-train space borne observations (CALIPSO and CLOUDSAT) to evaluate cloud models performance in selected areas.

Contact

M. Chiriaco

Acknowledgment

References

Beljaars, ACM. 1994. "The parameterization of surface fluxes in large-scale models under free convection." *Quarterly Journal of the Royal Meteorological Society* 121, 255-270.

Chiriaco, M, H Chepfer, V Noel, A Delaval, M Haeffelin, P Dubuisson, and P Yang. 2004. "Improving Retrievals of Cirrus Cloud Particle Size Coupling Lidar and Three-Channel Radiometric Techniques." *Monthly Weather Review* 132, 1684-1700.

Collis, RT, and PB Russel. 1976. "Laser Monitoring of the Atmosphere." Springer-Verlag, New York.

Dudhia, J. 1989. "Numerical Study of Convection Observed during the Winter Monsoon Experiment Using a Mesoscale Two-Dimensional Model." *Journal of Atmospheric Science* 46(20):3077-3107.

Grell, G. 1993. "Prognostic evaluation of assumptions used by cumulus parameterizations." *Monthly Weather Review* 121, 764-787.

Hack, JJ, BA Boville, BP Briegleb, JT Kiehl, PJ Rasch, and DL Williamson. 1993. Description of the NCAR Community Climate Model (CCM2). NCAR Tech. Note, NCAR/TN-382+STR, National Center for Atmospheric Research, Boulder, Colorado, pp. 108.

Haeffelin, M, L Barthès, O Bock, C Boitel, S Bony, B Bouniol, H Chepfer, M Chiriaco, J Delanoë, P Drobinski, JL Dufresne, C Flamant, M Grall, A Hodzic, F Hourdin, F Lapouge, Y Lemaître, A Mathieu, Y Morille, C Naud, V Noël, J Pelon, C Pietras, A Protat, B Romand, G Scialom, and R Vautard. 2004. "SIRTA, a ground-based atmospheric observatory for clouds and aerosols research." *Annales Geophysics* Accepted November 2004.

Heymsfield, AJ, and CMR Platt. 1984. "A parameterization of the particle size spectrum of ice clouds in term of the ambient temperature and the Ice Water Content." *Journal of Atmospheric Science* 41, 846-855.

Heymsfield, AJ, and LJ Donner. 1990. "A Scheme for Parameterizing Ice-Cloud Water Content in General Circulation Models." *Journal of Atmospheric Science* 47, 1865-1877.

Liou, KN. 1986. "Influence of cirrus clouds on weather and climate processes: A global perspective." *Monthly Weather Review* 114, 1167-1199

Liou, KN. 2002. "An Introduction to Atmospheric Radiation (International Geophysics Series)." Academic Press, pp. 175.

Minnis, P, DP Garber, and DF Young. 1998. "Parameterization of Reflectance and Effective Emittance for Satellite Remote Sensing of Cloud Properties." *Journal of Atmospheric Science* 55, 3313-3339.

Morille, Y, M Haeffelin, P Drobinski, and J Pelon. 2005. "STRAT: STRucture of the ATmosphere from single channel lidar data." *Submitted to Journal of Atmospheric and Oceanic Technology* In revision.

Noel, V, H Chepfer, G Ledanois, and PH Flamant. 2001. "Computation of single-scattering matrix for non-spherical particles randomly or horizontally oriented in space." *Applied Optics* 40, 4365-4375.

Noel, V, H Chepfer, G Ledanois, A Delaval, and PH Flamant. 2002. "Classification of Particle Effective Shape Ratios in Cirrus Clouds Based on Lidar Depolarization Ratio." *Applied Optics* 41(21):4245-4257.

Platt, CMR. 1973. "Lidar and Radiometric Observations of Cirrus clouds." *Journal of Atmospheric Science* 30, 1191-1204.

Protat, A, J Delanoë, D Bouniol, and M Haeffelin. 2004. Dynamical, microphysical and radiative properties of ice clouds using Doppler cloud radar measurements. Third European Radar Conference, September 6-10, 2004, Visbi, Sweden.

Reisner, J, RM Rasmussen, and RT Bruintjes. 1998. "Explicit forecasting of supercooled liquid water in winter storms using the MM5 mesoscale model." *Quarterly Journal of the Royal Meteorological Society* 124, 1071-1107.

Sassen, K. 1991. "The polarization lidar technique for cloud research: A review and current assessment." *Bulletin of the American Meteorological Society* 72, 1848-1866.

Troën, I, and L Mahrt. 1986. "A simple model of the atmospheric boundary. Sensitivity to surface evaporation." *Bound.-Layer Meteorology* 37, 129-148.

Ulaby, FT, RK Moore, and AK Fung. 1943. "Microwave Remote-Sensing active and passive." Vol. 1, Microwave Remote-Sensing Fundamentals and Radiometry. Artech House. INC Ed.

Zurovac-Jevtic, D, and GJ Zhang. 2003. "Development and Test of a Cirrus Parameterization Scheme Using NCAR CCM3." *Journal of Atmospheric Science* 60(11):1325-1344.